



OPEN

Hybridization of the swarming and interior point algorithms to solve the Rabinovich–Fabrikant system

Zulqurnain Sabir, Salem Ben Said & Qasem Al-Mdallal

In this study, a trustworthy swarming computing procedure is demonstrated for solving the nonlinear dynamics of the Rabinovich–Fabrikant system. The nonlinear system’s dynamic depends upon the three differential equations. The computational stochastic structure based on the artificial neural networks (ANNs) along with the optimization of global search swarming particle swarm optimization (PSO) and local interior point (IP) algorithms, i.e., ANNs-PSOIP is presented to solve the Rabinovich–Fabrikant system. An objective function based on the differential form of the model is optimized through the local and global search methods. The correctness of the ANNs-PSOIP scheme is observed through the performances of achieved and source solutions, while the negligible absolute error that is around 10^{-05} – 10^{-07} also represent the worth of the ANNs-PSOIP algorithm. Furthermore, the consistency of the ANNs-PSOIP scheme is examined by applying different statistical procedures to solve the Rabinovich–Fabrikant system.

A noteworthy Rabinovich–Fabrikant system based on the chaotic system was developed by the eminent scientists Rabinovich and Fabrikant. This is a condensed version of a nonlinear complex parabolic system that models various physical processes, like as wind waves on water, the hydrodynamic flows based on the Tollmien–Schlichting waves, Langmuir waves in plasma, concentration waves using the chemical reactions with diffusion. First, the model’s design is implemented in a physical system, which represent the modulation inconsistency using the medium of dissipative non-equilibrium^{1,2}. Currently, it has been acknowledged in the model’s extraordinarily high dynamics along with various physical features³. Notably, the Lorenz and other chaotic models are based on the nonlinearities of the second kind. Whereas the Rabinovich–Fabrikant system has the third kind of nonlinearities using some remarkable dynamics, that is “virtual” saddles combined with numerous chaotic charming characters with distinctive characteristics as well as mysterious chaotic fascinations^{4–11}. The systems having numerous dynamics that can exhibit the chaotic nonlinearities. The chaotic transients are established in the model and the chaotic transients have influential consequences for experimentations. To mention few of them are radio maps¹², circuits¹³, hydrodynamics¹⁴, Lorenz system¹⁵, neural networks¹⁶, and Rössler system¹⁷.

A significant challenge for intellectual researchers is provided by using the modelling based on the system of nonlinear equations and one of the Rabinovich–Fabrikant chaotic systems that comprises an ordinary three coupled differential equations using the pioneer work of M. Rabinovich and A. Fabrikant, given as^{2,18}:

$$\begin{cases} u'(\theta) = (u^2(\theta) + m(\theta) - 1)v(\theta) + eu(\theta), & u(0) = k_1, \\ v'(\theta) = (-u^2(\theta) + 3m(\theta) + 1)u(\theta) + ev(\theta), & v(0) = k_2, \\ m'(\theta) = -2(u(\theta)v(\theta) + f)m(\theta), & m(0) = k_3, \end{cases} \quad (1)$$

The above form of the nonlinear system has a variety of applications in various disciplines of mathematics and physics. k_1 , k_2 and k_3 are in the initial form of the conditions, where e and f indicate the real finite constant values based on the model’s evolution control.

The current research relates to the solutions of the Rabinovich–Fabrikant system using the computational stochastic artificial neural networks (ANNs) together with the global search swarming particle swarm optimization (PSO) and local interior point (IP) algorithms, i.e., ANNs-PSOIP. Recently, these stochastic performances have been represented to solve various nonlinear and stiff natured models^{19–25}, some of them are automated

Department of Mathematical Sciences, College of Science, United Arab Emirates University, P. O. Box 15551, Al Ain, UAE. email: salem.bensaid@uaeu.ac.ae

rail-mounted gantry crane model²⁶, heterogeneous-vehicle capacitated arc routing problem²⁷, drone-assisted camera network²⁸, triboelectric sensors for surface identification²⁹, thermal explosion system^{30,31}, traffic flow prediction³², biological kind of Leptospirosis system^{33,34}, high-dimensional expensive problems³⁵, food chain nonlinear differential systems^{36–38}, vector machine parameter optimization algorithm³⁹, functional kind of systems^{40,41}, wireless-powered systems⁴², singular nature nonlinear models^{43–46} and many more^{47–50}. To inspire of these stochastic applications, the authors took keen interest to perform the solutions of the Rabinovich–Fabrikant system through the swarming computational procedures. Some innovative features are itemized as:

- The numerical solutions of the Rabinovich–Fabrikant system are presented efficiently by applying the proposed ANNs along with the swarming computational procedure.
- The consistent, trustworthy, and steady outputs of this system authenticate the correctness of the designed ANNs together with a swarming computational scheme.
- The small calculate absolute error (AE) performs the accuracy of the ANNs together with the swarming computational approach.
- The authentication of the computational ANNs together with the swarming computational approach is established by taking three statistical operators with 50 executions to solve the model.

The rest of the presentation of the paper is given as: The procedure of the ANNs together with the swarming scheme is given in Section "Proposed ANNs-PSOIP method". The numerical solutions with different plots and tables are presented in Section "Result performances". The conclusions are drawn in the last Section.

Proposed ANNs-PSOIP method

The Rabinovich–Fabrikant system is solved numerically by applying the swarming computational procedures. The mathematical neural network formulations are shown as:

$$\begin{aligned}
 [\hat{u}(\theta), \hat{v}(\theta), \hat{m}(\theta)] &= \left[\sum_{i=1}^p q_{u,i} Y(w_{u,i}\theta + r_{u,i}), \sum_{i=1}^p q_{v,i} Y(w_{v,i}\theta + r_{v,i}), \sum_{i=1}^p q_{m,i} Y(w_{m,i}\theta + r_{m,i}) \right], \\
 [\hat{u}'(\theta), \hat{v}'(\theta), \hat{m}'(\theta)] &= \left[\sum_{i=1}^p q_{u,i} Y'(w_{u,i}\theta + r_{u,i}), \sum_{i=1}^p q_{v,i} Y'(w_{v,i}\theta + r_{v,i}), \sum_{i=1}^p q_{m,i} Y'(w_{m,i}\theta + r_{m,i}) \right],
 \end{aligned} \tag{2}$$

where, p , Y present the neurons and activation function, while the unknown weights W , shown as $W = [W_u, W_v, W_m]$, for $W_u = [q_u, \omega_u, r_u]$, $W_v = [q_v, \omega_v, r_v]$, and $W_m = [q_m, \omega_m, r_m]$, where

$$\begin{aligned}
 q_u &= [q_{u,1}, q_{u,2}, \dots, q_{u,p}], & q_v &= [q_{v,1}, q_{v,2}, \dots, q_{v,p}], & q_m &= [q_{m,1}, q_{m,2}, \dots, q_{m,p}], \\
 w_u &= [w_{u,1}, w_{u,2}, \dots, w_{u,p}], & w_v &= [w_{v,1}, w_{v,2}, \dots, w_{v,p}], & w_m &= [w_{m,1}, w_{m,2}, \dots, w_{m,p}], \\
 r_u &= [r_{u,1}, r_{u,2}, \dots, r_{u,p}], & r_v &= [r_{v,1}, r_{v,2}, \dots, r_{v,p}], & r_m &= [r_{m,1}, r_{m,2}, \dots, r_{m,p}].
 \end{aligned}$$

The mathematical form of the transfer log-sigmoid function is given as: $Y(\theta) = (1 + e^{-\theta})^{-1}$.

$$\begin{aligned}
 [\hat{u}(\theta), \hat{v}(\theta), \hat{m}(\theta)] &= \left[\sum_{i=1}^p \frac{q_{u,i}}{1 + e^{-(w_{u,i}\theta + r_{u,i})}}, \sum_{i=1}^p \frac{q_{v,i}}{1 + e^{-(w_{v,i}\theta + r_{v,i})}}, \sum_{i=1}^p \frac{q_{m,i}}{1 + e^{-(w_{m,i}\theta + r_{m,i})}} \right], \\
 [\hat{u}'(\theta), \hat{v}'(\theta), \hat{m}'(\theta)] &= \left[\sum_{i=1}^p \frac{q_{u,i} w_{u,i} e^{-(w_{u,i}\theta + r_{u,i})}}{(1 + e^{-(w_{u,i}\theta + r_{u,i})})^2}, \sum_{i=1}^p \frac{q_{v,i} w_{v,i} e^{-(w_{v,i}\theta + r_{v,i})}}{(1 + e^{-(w_{v,i}\theta + r_{v,i})})^2}, \sum_{i=1}^p \frac{q_{m,i} w_{m,i} e^{-(w_{m,i}\theta + r_{m,i})}}{(1 + e^{-(w_{m,i}\theta + r_{m,i})})^2} \right].
 \end{aligned} \tag{3}$$

A merit function is designed as:

$$e = \sum_{j=1}^4 e_j \tag{4}$$

$$e_1 = \frac{1}{N} \sum_{c=1}^N [\hat{u}'_c - (\hat{u}_c^2 + \hat{m}_c - 1)\hat{v}_c - e\hat{u}_c]^2, \tag{5}$$

$$e_2 = \frac{1}{N} \sum_{c=1}^N [\hat{v}_c - (-\hat{u}_c^2 + 3\hat{m}_c + 1)\hat{u}_c - e\hat{v}_c]^2, \tag{6}$$

$$e_3 = \frac{1}{N} \sum_{c=1}^N [\hat{m}'_c + 2(f + \hat{u}_c \hat{v}_c)\hat{m}_c]^2, \tag{7}$$

$$e_4 = \frac{1}{3} \left[(\hat{u}_0 - k_1)^2 + (\hat{v}_0 - k_2)^2 + (\hat{m}_0 - k_3)^2 \right], \tag{8}$$

where $\hat{u}_c = u(\theta_c)$, $\hat{v}_c = v(\theta_c)$, $\hat{m}_c = m(\theta_c)$, $Nh = 1$, and $\theta_c = hc$.

Optimization schemes. The optimizations through the PSOIP for solving the Rabinovich–Fabrikant system are presented in this section.

PSO is a global search neuro swarming scheme introduced by Kennedy and Eberhart in the previous century, which works as an alteration of genetic algorithm (GA)⁵¹. PSO exhibits the outcomes of multiple intricate systems that manage a specific population through the technique of optimum training. PSO works by using the minimum storage capacity⁵². In recent decades, PSO is used in various submissions, like as mixed-variable optimization systems⁵³, engineering networks⁵⁴, multi-objective multimodal approaches⁵⁵, solar form of the energy sets⁵⁶, photovoltaic parameters category based on single, dual and three-ways diode⁵⁷, studies of plant illnesses⁵⁸, image recognition⁵⁹, particle filter noise reduction based on mechanical accountability⁶⁰, and production systems using the green coal⁶¹. These remarkable proposals motivated the authors to operate the swarming approaches for the Rabinovich–Fabrikant system.

The global PSO process is considered a slow and sluggish scheme like the GA, which perform rapid convergence with the hybridization of the local search method. Consequently, IP approach is used by taking the primary inputs of the global PSO. IP is an outstanding scheme, which is applied to model the unconstrained/constrained systems. Some important IP applications are the shrinking horizon model predictive control with variable discretization step⁶², quantum key distribution rate computation⁶³, parameters estimation using the symmetric spinning projectiles based on the maximum likelihood scheme⁶⁴, equilibrium problems of the fisher market using the kernel function⁶⁵, and symmetric cone horizontal linear complementarity model using the function of positive-asymptotic barrier⁶⁶. The process of the swarming scheme along with a local search method to solve the Rabinovich–Fabrikant system is presented in Fig. 1.

Statistical measures. In this section, the statistical performances based on the semi-interquartile range (SIR), mean square error (MSE), and Theil’s inequality coefficient (TIC) are shown as:

$$\begin{cases} \text{SIR} = 0.5(Q_3 - Q_1), \\ Q_3 \ \& \ Q_1 = 3\text{rd} \ \& \ 1\text{st} \ \text{quartile}, \end{cases} \tag{9}$$

$$[\text{MSE}_u, \text{MSE}_v, \text{MSE}_m] = \left[\sum_{l=1}^m (u_l - \hat{u}_l)^2, \sum_{l=1}^m (v_l - \hat{v}_l)^2, \sum_{l=1}^m (m_l - \hat{m}_l)^2 \right], \tag{10}$$

$$[\text{TIC}_u, \text{TIC}_v, \text{TIC}_m] = \left[\frac{\sqrt{\frac{1}{n} \sum_{l=1}^n (u_l - \hat{u}_l)^2}}{\left(\sqrt{\frac{1}{n} \sum_{l=1}^n u_l^2} + \sqrt{\frac{1}{n} \sum_{l=1}^n \hat{u}_l^2} \right)}, \frac{\sqrt{\frac{1}{n} \sum_{l=1}^n (v_l - \hat{v}_l)^2}}{\left(\sqrt{\frac{1}{n} \sum_{l=1}^n v_l^2} + \sqrt{\frac{1}{n} \sum_{l=1}^n \hat{v}_l^2} \right)}, \frac{\sqrt{\frac{1}{n} \sum_{l=1}^n (m_l - \hat{m}_l)^2}}{\left(\sqrt{\frac{1}{n} \sum_{l=1}^n m_l^2} + \sqrt{\frac{1}{n} \sum_{l=1}^n \hat{m}_l^2} \right)} \right]. \tag{11}$$

Result performances

The numerical solutions of the Rabinovich–Fabrikant system (1) are presented by using the swarming computing procedures. The plots of results overlapping, weights, statistical performances along with the AE are also illustrated in this section. The system (1) is updated by using the suitable values as:

$$\begin{cases} u'(\theta) = (u^2(\theta) + m(\theta) - 1)v(\theta) + 2u(\theta), & u(0) = 0.1, \\ v'(\theta) = (-u^2(\theta) + 3m(\theta) + 1)u(\theta) + 2v(\theta), & v(0) = 0.2, \\ m'(\theta) = -2(u(\theta)v(\theta) + 3)m(\theta), & m(0) = 0.3. \end{cases} \tag{12}$$

A fitness function is shown as:

$$e = \frac{1}{N} \sum_{c=1}^N \left([\hat{u}'_c - (\hat{u}_c^2 + \hat{m}_c - 1)\hat{v}_c - e\hat{u}_c]^2 + [\hat{v}_c - (-\hat{u}_c^2 + 3\hat{m}_c + 1)\hat{u}_c - e\hat{v}_c]^2 + [\hat{m}'_c + 2(f + \hat{u}_c\hat{v}_c)\hat{m}_c]^2 \right) + \frac{1}{3} \left[(\hat{u}_0 - 0.1)^2 + (\hat{v}_0 - 0.2)^2 + (\hat{m}_0 - 0.3)^2 \right]. \tag{13}$$

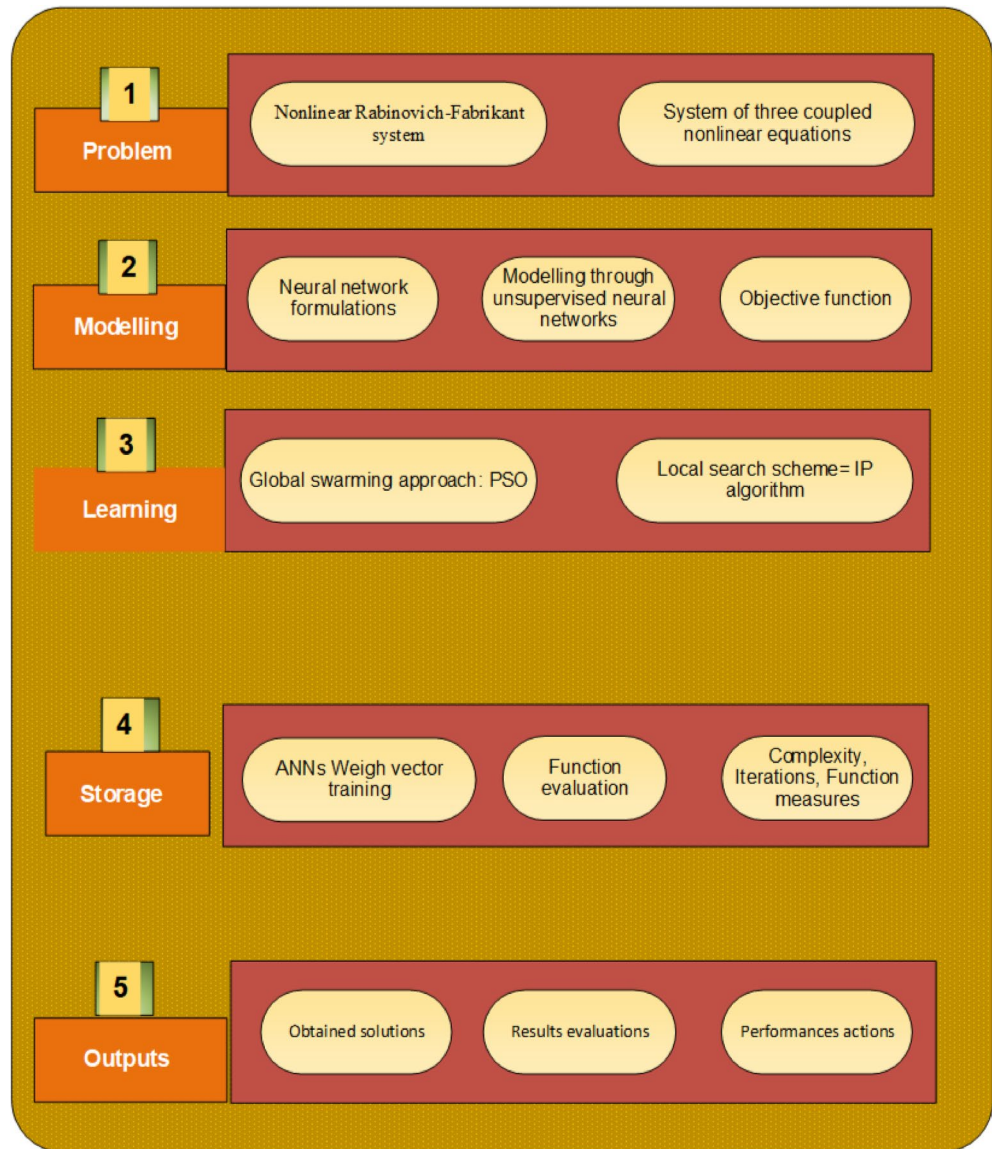


Figure 1. Designed swarming and local search procedures to solve the Rabinovich–Fabrikant system.

The optimization of objective function given in system (13) is provided by using the ANNs together with the swarming computational approach to solve the Rabinovich–Fabrikant system. Ten numbers of neurons along with 50 runs have been executed to check the reliability of the procedure. The optimal results based on the weight vectors for solving the above system are shown below.

$$\hat{u}(\theta) = \frac{0.0042}{1 + e^{-(7.3325\theta - 5.1850)}} - \frac{5.5634}{1 + e^{-(13.460\theta + 19.964)}} - \frac{0.3437}{1 + e^{-(2.8283\theta - 1.7191)}} - \frac{5.6722}{1 + e^{-(1.1198\theta - 10.419)}} \\ + \frac{0.1638}{1 + e^{-(3.7726\theta + 2.1030)}} + \frac{2.5293}{1 + e^{-(5.277\theta - 6.3198)}} - \frac{0.2724}{1 + e^{-(21.008\theta - 26.939)}} + \frac{5.4190}{1 + e^{-(4.135\theta + 5.0166)}} \\ + \frac{0.9113}{1 + e^{-(1.7256\theta - 1.3888)}} - \frac{2.5793}{1 + e^{-(4.3167\theta - 11.933)}}, \quad (14)$$

$$\hat{v}(\theta) = \frac{13.6431}{1 + e^{-(10.727\theta + 20.281)}} - \frac{0.0229}{1 + e^{-(1.5494\theta + 5.9631)}} - \frac{5.8231}{1 + e^{-(6.3142\theta + 9.5120)}} - \frac{5.0170}{1 + e^{-(0.316\theta + 3.209)}} \\ - \frac{2.3954}{1 + e^{-(0.437\theta + 0.2973)}} - \frac{1.4387}{1 + e^{-(3.303\theta + 2.755)}} - \frac{7.3507}{1 + e^{-(7.8204\theta - 9.816)}} + \frac{2.3850}{1 + e^{-(0.8992\theta - 9.8543)}} \\ - \frac{4.9011}{1 + e^{-(13.757\theta - 27.113)}} - \frac{0.0487}{1 + e^{-(1.2584\theta + 4.4397)}}, \quad (15)$$

$$\hat{m}(\theta) = \frac{-1.2311}{1 + e^{-(3.8031\theta - 3.0875)}} - \frac{1.6094}{1 + e^{-(7.3334\theta - 2.0239)}} - \frac{2.2478}{1 + e^{-(2.5328\theta - 2.8606)}} + \frac{2.1662}{1 + e^{-(5.0115\theta - 2.3467)}} \\ - \frac{0.3374}{1 + e^{-(6.173\theta - 2.5454)}} - \frac{6.8904}{1 + e^{-(7.844\theta - 12.2045)}} + \frac{6.2610}{1 + e^{-(7.642\theta - 2.7489)}} - \frac{5.3609}{1 + e^{-(2.1072\theta - 6.2498)}} \\ + \frac{5.0547}{1 + e^{-(2.4580\theta - 3.7097)}} + \frac{5.3493}{1 + e^{-(1.9603\theta - 6.1331)}}, \quad (16)$$

Figure 2 illustrates the values of the optimal weights along with the result's assessment for each class of the Rabinovich–Fabrikant system. These weights are shown in Fig. 2a–c by applying the ANNs together with the swarming computational approach to solve the Rabinovich–Fabrikant system by taking 10 numbers of neurons. The correctness of the ANNs together with the swarming and local computational method is examined through the best, reference and mean results in Fig. 2d–f. Figure 3 shows the mean and best results based on the AE to solve the Rabinovich–Fabrikant system. The best AE measures are performed as 10^{-04} – 10^{-07} , 10^{-05} – 10^{-07} and 10^{-06} – 10^{-07} , while the mean values of the AE are performed as 10^{-02} – 10^{-03} , 10^{-01} to 10^{-03} and 10^{-03} – 10^{-04} for 1st–3rd dynamics. These reduceable performances of AE improve the precision of the ANNs. Figure 4 represents the performances of TIC that have been calculated based on the Rabinovich–Fabrikant system, which are found around 10^{-06} – 10^{-10} for each category. The MSE values are plotted in Fig. 5 to solve the Rabinovich–Fabrikant system through the stochastic approach. These performances are described as 10^{-04} – 10^{-10} for the system. The optimal statistical performances achieved through the ANNs together with the swarming scheme develop the method's consistency to solve the above system.

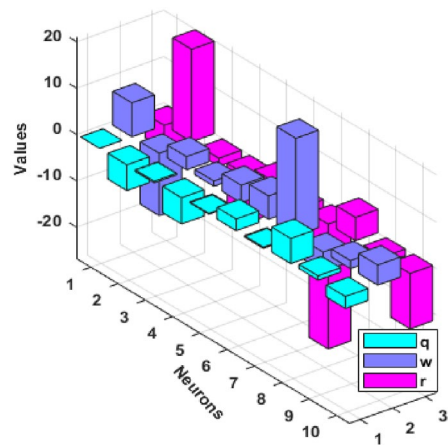
Tables 1, 2, 3 shows the statistical operator measures for the minimum (best results), SIR, mean, maximum (worst outputs), median, and standard deviation (SD) values. The plots based on the maximum performances (bad results) reported as 10^{-01} – 10^{-02} for the first two dynamics of the model, while these values performed as 10^{-03} – 10^{-04} for the last dynamic of the model. The mean and SD operator values are 10^{-02} – 10^{-03} and 10^{-01} – 10^{-02} for the first two dynamics, while these values lie as 10^{-04} – 10^{-05} for the last dynamic of the model. Likewise, the median, minimum (best performances) and SIR operator values for each class of the Rabinovich–Fabrikant system are found as 10^{-04} – 10^{-05} , 10^{-06} – 10^{-07} and 10^{-03} – 10^{-05} . Based on these performances, the process of the ANNs together with the swarming and local search scheme perform precise to solve the Rabinovich–Fabrikant system.

Conclusions

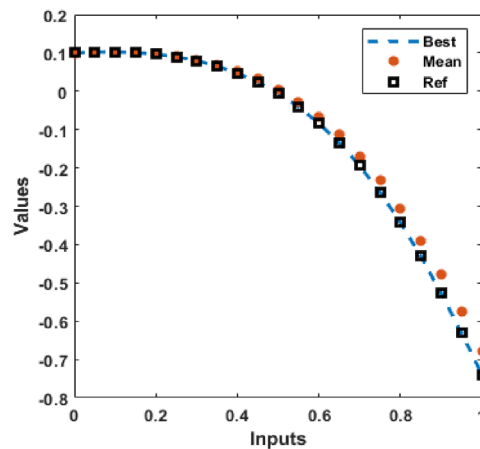
The current investigations present a stochastic computing reliable scheme based on the swarming computing procedure for the numerical solutions of the Rabinovich–Fabrikant system. The system's dynamic of the nonlinear system has three coupled equations. Some of the concluding remarks are itemized as:

- The computing stochastic artificial neural networks along with the global swarming and local search interior point algorithms have been presented to solve the differential form of the Rabinovich–Fabrikant system.
- The design of objective function has been presented by using the differential system, while the optimization is performed through the local and global search schemes.
- The accuracy of the results has been observed through the achieved and source results performances.
- The log-sigmoid transfer function along with 10 numbers of neurons in the structure of neural network have been provided for the solutions of the Rabinovich–Fabrikant system.
- The absolute error has also been achieved around 10^{-05} – 10^{-08} , which shows the worth of the ANNs-PSOIP algorithm.
- The consistency of the ANNs-PSOIP method has been examined by applying different statistical performances to solve the Rabinovich–Fabrikant system.

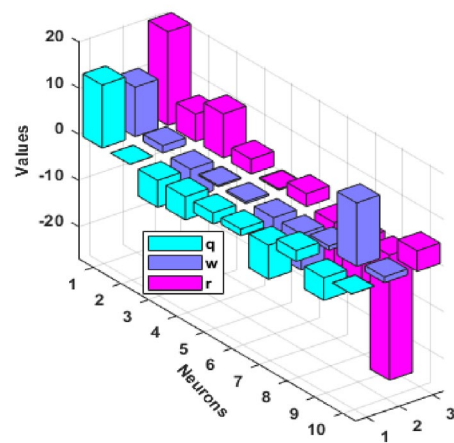
In future, the designed ANNs along with the swarming scheme is provided to perform the solutions of the biological system^{67,68}, and fluid dynamical systems⁶⁹.



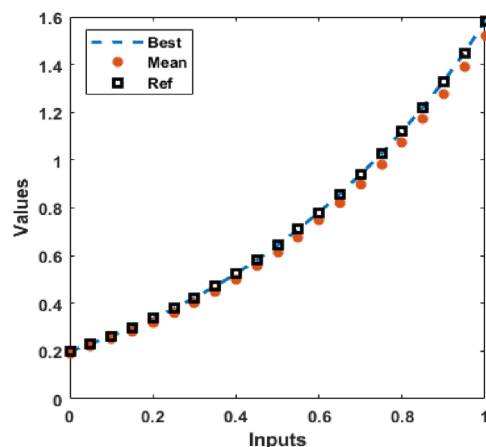
(a) Weights $u(\theta)$



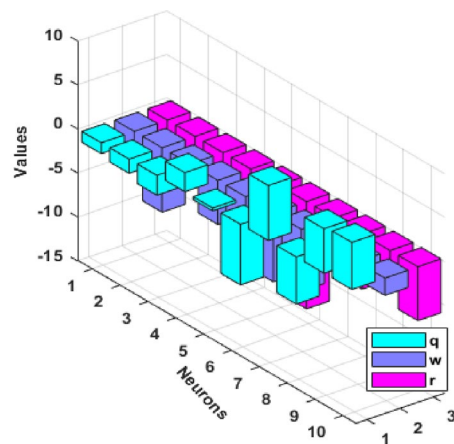
(d) Results $u(\theta)$



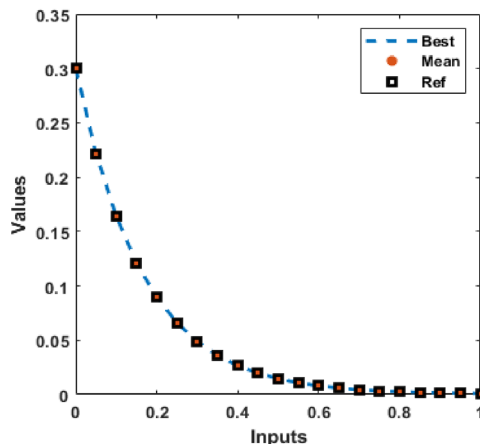
(b) Weights $v(\theta)$



(e) Results of $v(\theta)$

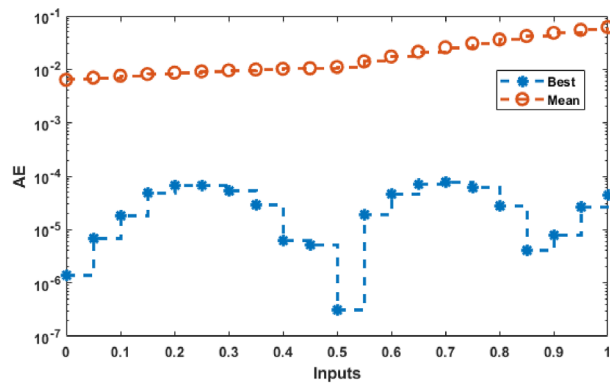


(c) Weights $m(\theta)$

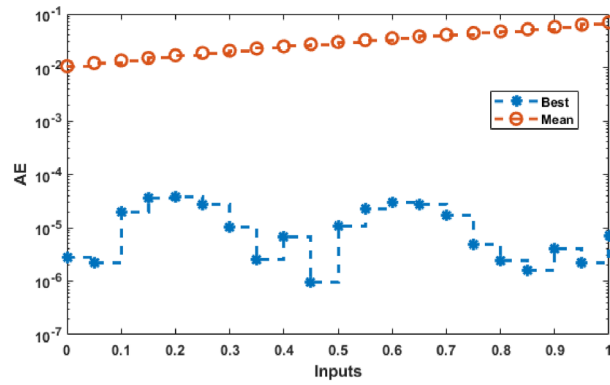


(f) Results $m(\theta)$

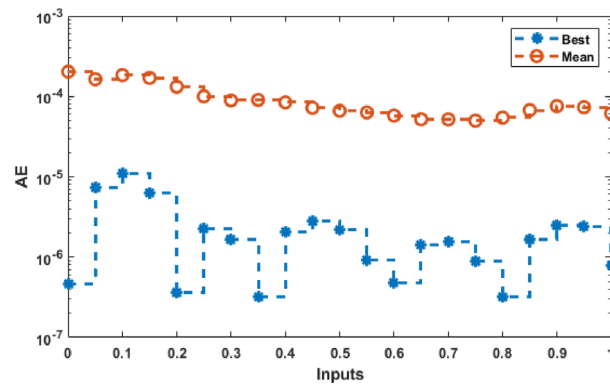
Figure 2. Weights and comparison of solution performances for the Rabinovich–Fabrikant system.



(a) AE for the class $u(\theta)$



(b) AE for the class $v(\theta)$



(c) AE for the class $m(\theta)$

Figure 3. The values of AE to solve the Rabinovich–Fabrikant system.

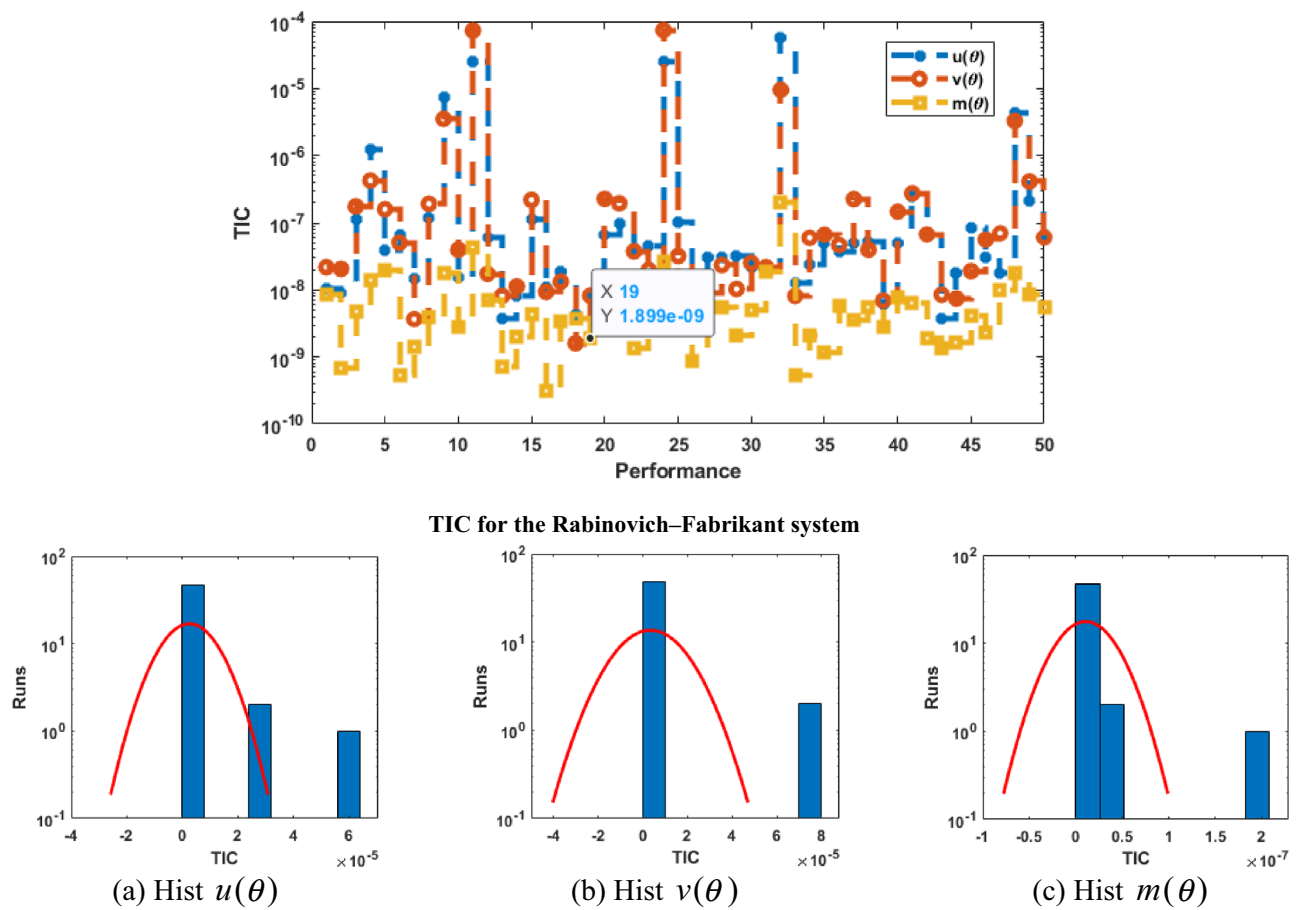


Figure 4. Performances of TIC along with hist values for the mathematical system.

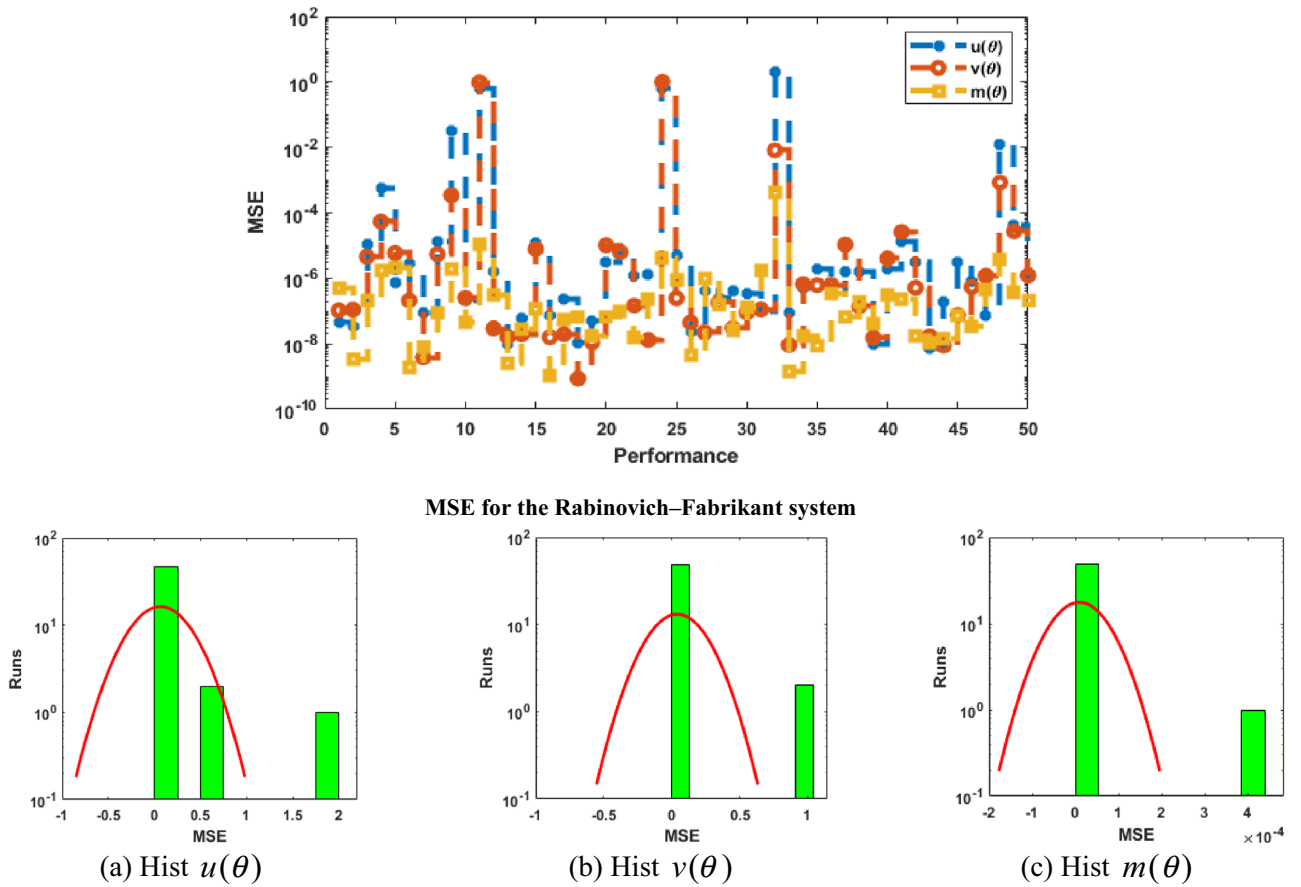


Figure 5. Performances of MSE along with hist values for the mathematical system.

θ	$u(\theta)$					
	Maximum	Mean	Median	Minimum	SD	SIR
0	1.05690E-01	6.40790E-03	5.08468E-05	1.20218E-06	2.36816E-02	7.58571E-05
0.05	1.22841E-01	6.98814E-03	4.02634E-05	3.18951E-07	2.57846E-02	6.18554E-05
0.1	1.43050E-01	7.57637E-03	6.17875E-05	1.37938E-06	2.79626E-02	7.98119E-05
0.15	1.66086E-01	8.15105E-03	1.22617E-04	1.77658E-07	3.02299E-02	9.80690E-05
0.2	1.91909E-01	8.69372E-03	1.73347E-04	3.56693E-06	3.26824E-02	1.13967E-04
0.25	2.20686E-01	9.18423E-03	2.17530E-04	1.40996E-06	3.54503E-02	1.42554E-04
0.3	2.52773E-01	9.61410E-03	2.08632E-04	3.07849E-06	3.86938E-02	1.73721E-04
0.35	2.88683E-01	9.97919E-03	1.76354E-04	2.72037E-05	4.26073E-02	2.25364E-04
0.4	3.29034E-01	1.02867E-02	1.96363E-04	6.17216E-06	4.74130E-02	1.49917E-04
0.45	3.74495E-01	1.05397E-02	2.16955E-04	4.38184E-06	5.33532E-02	1.86919E-04
0.5	4.25732E-01	1.11452E-02	2.59888E-04	3.07209E-07	6.05991E-02	2.54918E-04
0.55	4.83354E-01	1.40952E-02	3.45508E-04	6.56680E-07	6.90186E-02	3.67314E-04
0.6	5.47875E-01	1.75133E-02	4.05529E-04	4.48314E-05	7.91777E-02	4.12311E-04
0.65	6.19674E-01	2.14188E-02	4.85687E-04	6.63475E-05	9.12644E-02	4.99647E-04
0.7	6.98962E-01	2.58265E-02	4.88451E-04	5.95039E-05	1.05424E-01	5.17867E-04
0.75	7.85725E-01	3.07458E-02	4.66624E-04	2.26947E-05	1.21745E-01	5.64742E-04
0.8	8.79659E-01	3.61768E-02	4.81259E-04	2.30813E-05	1.40240E-01	5.81885E-04
0.85	9.80067E-01	4.21008E-02	5.43547E-04	4.09488E-06	1.60816E-01	6.03728E-04
0.9	1.08574E-01	4.84540E-02	6.14579E-04	7.74713E-06	1.83256E-01	7.85763E-04
0.95	1.19485E-01	5.51122E-02	7.79590E-04	1.55711E-06	2.07173E-01	6.99057E-04
1	1.30480E-01	6.17905E-02	8.51394E-04	1.89442E-06	2.32010E-01	7.90777E-04

Table 1. Different statistical measures for the Rabinovich–Fabrikant system (1).

θ	$v(\theta)$					
	Maximum	Mean	Median	Minimum	SD	SIR
0	1.80930E-01	1.05117E-02	1.56302E-04	1.20218E-06	3.85499E-02	2.28766E-04
0.05	2.16171E-01	1.20503E-02	1.78333E-04	3.18951E-07	4.49069E-02	2.85149E-04
0.1	2.49110E-01	1.35299E-02	1.75805E-04	1.37938E-06	5.12729E-02	3.03159E-04
0.15	2.84048E-01	1.50777E-02	1.89514E-04	1.77658E-07	5.80619E-02	3.11228E-04
0.2	3.23084E-01	1.67597E-02	2.18140E-04	3.56693E-06	6.55171E-02	3.24209E-04
0.25	3.65827E-01	1.85756E-02	2.48140E-04	1.40996E-06	7.36480E-02	4.01238E-04
0.3	4.12074E-01	2.05200E-02	2.79358E-04	3.07849E-06	8.24701E-02	4.84476E-04
0.35	4.61942E-01	2.25962E-02	2.83904E-04	2.72037E-05	9.20213E-02	5.49853E-04
0.4	5.15676E-01	2.48089E-02	2.86481E-04	6.17216E-06	1.02348E-01	6.16102E-04
0.45	5.73546E-01	2.71609E-02	3.19916E-04	4.38184E-06	1.13500E-01	5.65715E-04
0.5	6.35804E-01	2.96547E-02	2.79361E-04	3.07209E-07	1.25519E-01	6.06080E-04
0.55	7.02671E-01	3.23225E-02	3.10564E-04	6.56680E-07	1.38442E-01	8.43722E-04
0.6	7.74346E-01	3.51264E-02	3.57440E-04	4.48314E-05	1.52317E-01	9.45295E-04
0.65	8.51024E-01	3.80537E-02	4.28832E-04	6.63475E-05	1.67193E-01	1.03409E-03
0.7	9.32931E-01	4.10722E-02	5.16832E-04	5.95039E-05	1.83134E-01	1.12184E-03
0.75	1.02040E-01	4.41658E-02	5.67579E-04	2.26947E-05	2.00230E-01	1.20797E-03
0.8	1.11397E-01	4.73450E-02	5.75595E-04	2.30813E-05	2.18615E-01	1.26351E-03
0.85	1.21454E-01	5.17237E-02	5.70407E-04	4.09488E-06	2.38257E-01	1.33663E-03
0.9	1.32354E-01	5.70127E-02	5.87427E-04	7.74713E-06	2.59548E-01	1.46495E-03
0.95	1.44317E-01	6.29763E-02	6.95371E-04	1.55711E-06	2.83011E-01	1.72981E-03
1	1.57650E-01	6.97606E-02	8.67320E-04	1.89442E-06	3.09254E-01	1.98607E-03

Table 2. Different statistical measures for the Rabinovich–Fabrikant system (2).

θ	$m(\theta)$					
	Maximum	Mean	Median	Minimum	SD	SIR
0	6.58629E-03	2.02783E-04	1.55765E-05	1.20218E-06	9.33476E-04	2.82452E-05
0.05	5.01335E-03	1.63321E-04	3.64540E-05	3.18951E-07	7.04530E-04	3.23278E-05
0.1	3.95453E-03	1.83999E-04	5.27212E-05	1.37938E-06	5.58475E-04	5.83354E-05
0.15	3.17549E-03	1.69807E-04	5.08574E-05	1.77658E-07	4.57572E-04	6.92912E-05
0.2	2.56724E-03	1.31963E-04	2.40379E-05	3.56693E-06	3.77014E-04	4.77252E-05
0.25	2.07883E-03	9.98185E-05	1.84659E-05	1.40996E-06	3.10152E-04	3.22076E-05
0.3	1.68442E-03	8.91099E-05	3.09639E-05	3.07849E-06	2.56272E-04	2.17263E-05
0.35	1.36831E-03	9.03436E-05	3.79007E-05	2.72037E-05	2.13215E-04	2.64122E-05
0.4	1.11868E-03	8.42805E-05	2.71341E-05	6.17216E-06	1.80472E-04	3.13689E-05
0.45	9.25173E-04	7.17091E-05	2.33858E-05	4.38184E-06	1.54250E-04	2.63757E-05
0.5	7.77852E-04	6.60226E-05	2.41276E-05	3.07209E-07	1.28257E-04	2.95578E-05
0.55	6.68033E-04	6.31421E-05	3.93428E-05	6.56680E-07	1.05745E-04	2.73639E-05
0.6	5.87681E-04	5.76348E-05	3.32827E-05	4.48314E-05	9.08890E-05	2.44285E-05
0.65	5.29980E-04	5.17476E-05	2.58827E-05	6.63475E-05	8.24802E-05	2.16873E-05
0.7	4.89313E-04	5.16222E-05	3.40469E-05	5.95039E-05	7.67325E-05	2.12499E-05
0.75	4.61136E-04	4.97995E-05	2.54209E-05	2.26947E-05	7.96171E-05	1.61246E-05
0.8	4.41978E-04	5.43080E-05	1.88782E-05	2.30813E-05	8.53107E-05	2.74754E-05
0.85	4.29426E-04	6.73073E-05	3.04463E-05	4.09488E-06	8.79037E-05	3.25790E-05
0.9	4.21844E-04	7.54484E-05	4.33264E-05	7.74713E-06	9.04288E-05	3.38840E-05
0.95	4.18417E-04	7.30378E-05	4.63993E-05	1.55711E-06	9.43253E-05	2.54015E-05
1	4.19007E-04	6.14300E-05	1.74213E-05	1.89442E-06	1.04388E-04	2.89049E-05

Table 3. Different statistical measures for the Rabinovich–Fabrikant system (3).

Data availability

The datasets generated/produced during and/or analyzed during the current study/research are available from the corresponding author on reasonable request.

Received: 28 February 2023; Accepted: 22 June 2023

Published online: 06 July 2023

References

- Razaq, A., Ahmad, M. & El-Latif, A. A. A novel algebraic construction of strong S-boxes over double GF (27) structures and image protection. *Comput. Appl. Math.* **42**(2), 90 (2023).
- Rabinovich, M. I. & Fabrikant, A. L. Stochastic self-modulation of waves in nonequilibrium media. *J. Exp. Theor. Phys* **77**, 617–629 (1979).
- Danca, M. F., Feckan, M., Kuznetsov, N. & Chen, G. Looking more closely at the Rabinovich–Fabrikant system. *Int. J. Bifurcation Chaos* **26**(02), 1650038 (2016).
- Motsa, S.S., Dlamini, P.G. & Khumalo, M. Solving hyperchaotic systems using the spectral relaxation method. *Abstract and Applied Analysis*. **2012**, 18 (2012).
- Liu, Y., Yang, Q. & Pang, G. A hyperchaotic system from the Rabinovich system. *J. Comput. Appl. Math.* **234**(1), 101–113 (2010).
- Agrawal, S. K., Srivastava, M. & Das, S. Synchronization between fractional-order Rabinovich–Fabrikant and Lotka–Volterra systems. *Nonlinear Dyn.* **69**, 2277–2288 (2012).
- Chairez, I. Multiple DNN identifier for uncertain nonlinear systems based on Takagi–Sugeno inference. *Fuzzy Sets Syst.* **237**, 118–135 (2014).
- Zhang, C. X., Yu, S. M. & Zhang, Y. Design and realization of multi-wing chaotic attractors via switching control. *Int. J. Mod. Phys. B* **25**(16), 2183–2194 (2011).
- Srivastava, M., Agrawal, S. K., Vishal, K. & Das, S. Chaos control of fractional order Rabinovich–Fabrikant system and synchronization between chaotic and chaos controlled fractional order Rabinovich–Fabrikant system. *Appl. Math. Model.* **38**(13), 3361–3372 (2014).
- Danca, M. F., Kuznetsov, N. & Chen, G. Unusual dynamics and hidden attractors of the Rabinovich–Fabrikant system. *Nonlinear Dyn.* **88**, 791–805 (2017).
- Serrano-Guerrero, H., Cruz-Hernández, C., López-Gutiérrez, R. M., Cardoza-Avendaño, L. & ChávezPérez, R. A. Chaotic synchronization in nearest-neighbor coupled networks of 3D CNNs. *J. Appl. Res. Technol.* **11**(1), 26–41 (2013).
- Astafev, G. B., Koronovskii, A. A. & Khramov, A. E. Behavior of dynamical systems in the regime of transient chaos. *Tech. Phys. Lett.* **29**, 923–926 (2003).
- Zhu, L., Raghu, A. & Lai, Y. C. Experimental observation of superpersistent chaotic transients. *Phys. Rev. Lett.* **86**(18), 4017 (2001).
- Ahlers, G. & Walden, R. W. Turbulence near onset of convection. *Phys. Rev. Lett.* **44**(7), 445 (1980).
- Vadasz, P. Analytical prediction of the transition to chaos in Lorenz equations. *Appl. Math. Lett.* **23**(5), 503–507 (2010).
- Chen, L. & Aihara, K. Chaotic simulated annealing by a neural network model with transient chaos. *Neural Netw.* **8**(6), 915–930 (1995).
- Dhamala, M., Lai, Y. C. & Kostelich, E. J. Analyses of transient chaotic time series. *Phys. Rev. E* **64**(5), 056207 (2001).
- Moaddy, K., Freihat, A., Al-Smadi, M., Abuteen, E. & Hashim, I. Numerical investigation for handling fractional-order Rabinovich–Fabrikant model using the multistep approach. *Soft. Comput.* **22**(3), 773–782 (2018).
- Cao, B., Zhao, J., Lv, Z. & Yang, P. Diversified personalized recommendation optimization based on mobile data. *IEEE Trans. Intell. Transp. Syst.* **22**(4), 2133–2139 (2020).
- Zhu, H. & Zhao, R. Isolated Ni atoms induced edge stabilities and equilibrium shapes of CVD-prepared hexagonal boron nitride on the Ni (111) surface. *New J. Chem.* **46**(36), 17496–17504 (2022).
- Cao, B. *et al.* Large-scale many-objective deployment optimization of edge servers. *IEEE Trans. Intell. Transp. Syst.* **22**(6), 3841–3849 (2021).
- Cao, B., Sun, Z., Zhang, J. & Gu, Y. Resource allocation in 5G IoV architecture based on SDN and fog-cloud computing. *IEEE Trans. Intell. Transp. Syst.* **22**(6), 3832–3840 (2021).
- Ni, Q., Guo, J., Wu, W. and Wang, H., 2022. Influence-based community partition with sandwich method for social networks. *IEEE Trans. Comput. Soc. Syst.*
- Wang, H. *et al.* A structural evolution-based anomaly detection method for generalized evolving social networks. *Comput. J.* **65**(5), 1189–1199 (2022).
- Lu, B., Fan, C. R., Liu, L., Wen, K. & Wang, C. Speed-up coherent Ising machine with a spiking neural network. *Opt. Express* **31**(3), 3676–3684 (2023).
- Zhang, Y., Huang, Y., Zhang, Z., Postolache, O. & Mi, C. A vision-based container position measuring system for ARMG. *Meas. Control* **56**(3–4), 596–605 (2023).
- Cao, B. *et al.* A memetic algorithm based on two_Arch2 for multi-depot heterogeneous-vehicle capacitated arc routing problem. *Swarm Evol. Comput.* **63**, 100864 (2021).
- Cao, B. *et al.* Many-objective deployment optimization for a drone-assisted camera network. *IEEE Trans. Netw. Sci. Eng.* **8**(4), 2756–2764 (2021).
- Hou, X. *et al.* A space crawling robotic bio-paw (SCRBP) enabled by triboelectric sensors for surface identification. *Nano Energy* **105**, 108013 (2023).
- Sabir, Z. Neuron analysis through the swarming procedures for the singular two-point boundary value problems arising in the theory of thermal explosion. *Eur. Phys. J. Plus* **137**(5), 638 (2022).
- Sabir, Z. & Said, S. B. Heuristic computing for the novel singular third order perturbed delay differential model arising in thermal explosion theory. *Arab. J. Chem.* **16**(3), 104509 (2023).
- Zhang, X., Wen, S., Yan, L., Feng, J. & Xia, Y. A hybrid-convolution spatial-temporal recurrent network for traffic flow prediction. *Comput. J.* <https://doi.org/10.1093/comjnl/bxac171> (2022).
- Mukdasai, K. *et al.* A numerical simulation of the fractional order Leptospirosis model using the supervise neural network. *Alex. Eng. J.* **61**(12), 12431–12441 (2022).
- Botmart, T. *et al.* A hybrid swarming computing approach to solve the biological nonlinear Leptospirosis system. *Biomed. Signal Process. Control* **77**, 103789 (2022).
- Tian, J., Hou, M., Bian, H. & Li, J. Variable surrogate model-based particle swarm optimization for high-dimensional expensive problems. *Complex Intell. Syst.* <https://doi.org/10.1007/s40747-022-00910-7> (2022).
- Sabir, Z. Stochastic numerical investigations for nonlinear three-species food chain system. *Int. J. Biomath.* **15**(04), 2250005 (2022).
- Sabir, Z., Ali, M. R. & Sadat, R. Gudermannian neural networks using the optimization procedures of genetic algorithm and active set approach for the three-species food chain nonlinear model. *J. Ambient Intell. Humaniz. Comput.* **14**, 8913–8922 (2022).
- Souayah, B., Sabir, Z., Umar, M. & Alam, M. W. Supervised neural network procedures for the novel fractional food supply model. *Fractal Fractional* **6**(6), 333 (2022).

39. Li, X. & Sun, Y. Stock intelligent investment strategy based on support vector machine parameter optimization algorithm. *Neural Comput. Appl.* **32**, 1765–1775 (2020).
40. Sabir, Z., Guirao, J. L. & Saeed, T. Solving a novel designed second order nonlinear Lane-Emden delay differential model using the heuristic techniques. *Appl. Soft Comput.* **102**, 107105 (2021).
41. Guirao, J. L., Sabir, Z. & Saeed, T. Design and numerical solutions of a novel third-order nonlinear Emden-Fowler delay differential model. *Math. Probl. Eng.* <https://doi.org/10.1155/2020/7359242> (2020).
42. Cao, K. *et al.* Achieving reliable and secure communications in wireless-powered NOMA systems. *IEEE Trans. Veh. Technol.* **70**(2), 1978–1983 (2021).
43. Sabir, Z., Wahab, H. A. & Guirao, J. L. A novel design of Gudermannian function as a neural network for the singular nonlinear delayed, prediction and pantograph differential models. *Math. Biosci. Eng.* **19**(1), 663–687 (2022).
44. Sabir, Z., Said, S. B. & Baleanu, D. Swarming optimization to analyze the fractional derivatives and perturbation factors for the novel singular model. *Chaos Solitons Fractals* **164**, 112660 (2022).
45. Sabir, Z., Said, S. B., Al-Mdallal, Q. & Ali, M. R. A neuro swarm procedure to solve the novel second order perturbed delay Lane-Emden model arising in astrophysics. *Sci. Rep.* **12**(1), 22607 (2022).
46. Sabir, Z. *et al.* Dynamics of multi-point singular fifth-order Lane-Emden system with neuro-evolution heuristics. *Evol. Syst.* **13**, 795–806 (2022).
47. Li, H., *et al.* 2020. RS-MetaNet: Deep meta metric learning for few-shot remote sensing scene classification. Preprint at [arXiv:2009.13364](https://arxiv.org/abs/2009.13364).
48. Xie, X., Xie, B., Cheng, J., Chu, Q. & Dooling, T. A simple Monte Carlo method for estimating the chance of a cyclone impact. *Nat. Hazards* **107**, 2573–2582 (2021).
49. Xie, X., Tian, Y. & Wei, G. Deduction of sudden rainstorm scenarios: Integrating decision makers' emotions, dynamic Bayesian network and DS evidence theory. *Nat. Hazards* **116**, 2935–2955 (2023).
50. Liu, M. *et al.* Kinematics model optimization algorithm for six degrees of freedom parallel platform. *Appl. Sci.* **13**(5), 3082 (2023).
51. Shi, Y., & Eberhart, R. C. Empirical study of particle swarm optimization. In *Proceedings of the 1999 Congress on Evolutionary Computation-CEC99*, vol. 3, pp. 1945–1950, (IEEE, 1999).
52. Engelbrecht, A. P. *Computational Intelligence: An Introduction* 2nd edn. (John Wiley & Sons Ltd., 2007).
53. Liu, Y. & Wang, H. Surrogate-assisted hybrid evolutionary algorithm with local estimation of distribution for expensive mixed-variable optimization problems. *Appl. Soft Comput.* **133**, 109957 (2023).
54. De Almeida, B.S.G., & Leite, V.C. Particle swarm optimization: A powerful technique for solving engineering problems. *Swarm intelligence-recent advances, new perspectives and applications*, pp.1–21 (2019).
55. Zhang, X., Liu, H. & Tu, L. A modified particle swarm optimization for multimodal multi-objective optimization. *Eng. Appl. Artif. Intell.* **95**, 103905 (2020).
56. Elsheikh, A. H. & Abd Elaziz, M. Review on applications of particle swarm optimization in solar energy systems. *Int. J. Environ. Sci. Technol.* **16**(2), 1159–1170 (2019).
57. Youri, D., Thanikanti, S. B., Allam, D., Ramachandaramurthy, V. K. & Eteiba, M. B. Fractional chaotic ensemble particle swarm optimizer for identifying the single, double, and three diode photovoltaic models' parameters. *Energy* **195**, 116979 (2020).
58. Darwish, A., Ezzat, D. & Hassanien, A. E. An optimized model based on convolutional neural networks and orthogonal learning particle swarm optimization algorithm for plant diseases diagnosis. *Swarm Evol. Comput.* **52**, 100616 (2020).
59. Junior, F. E. F. & Yen, G. G. Particle swarm optimization of deep neural networks architectures for image classification. *Swarm Evol. Comput.* **49**, 62–74 (2019).
60. Chen, H. *et al.* Particle swarm optimization algorithm with mutation operator for particle filter noise reduction in mechanical fault diagnosis. *Int. J. Pattern Recognit Artif Intell.* **34**(10), 2058012 (2020).
61. Cui, Z. *et al.* Hybrid many-objective particle swarm optimization algorithm for green coal production problem. *Inf. Sci.* **518**, 256–271 (2020).
62. Zhang, Z., Zhao, Q. & Dai, F. A. A warm-start strategy in interior point methods for shrinking horizon model predictive control with variable discretization step. *IEEE Trans. Autom. Control.* **68**, 3830 (2022).
63. Hu, H., Im, J., Lin, J., Lütkenhaus, N. & Wolkowicz, H. Robust interior point method for quantum key distribution rate computation. *Quantum* **6**, 792 (2022).
64. Ying, W., Sun, S. & Wang, X. Parameters estimation for symmetric spinning projectiles using maximum likelihood method based on interior point algorithm. In *International Conference on Automation Control, Algorithm, and Intelligent Bionics (ACAIB 2022)* (Vol. 12253, pp. 216–224). (SPIE, 2022)
65. Chi, X., Yang, Q., Wan, Z. & Zhang, S. The new full-Newton step interior-point algorithm for the Fisher market equilibrium problems based on a kernel function. *J. Ind. Manag. Optim.* **19**, 7018–7035 (2023).
66. Asadi, S., Mahdavi-Amiri, N., Darvay, Z. & Rigó, P. R. Full Nesterov-Todd step feasible interior-point algorithm for symmetric cone horizontal linear complementarity problem based on a positive-asymptotic barrier function. *Optim. Methods Softw.* **37**(1), 192–213 (2022).
67. Guerrero-Sánchez, Y. *et al.* Solving a class of biological HIV infection model of latently infected cells using heuristic approach. *Discrete Contin. Dyn. Syst.-S.* **14**(10), 3611–3628. <https://doi.org/10.3934/dcds.2020431> (2021).
68. Trejos, D. Y., Valverde, J. C. & Venturino, E. Dynamics of infectious diseases: A review of the main biological aspects and their mathematical translation. *Appl. Math. Nonlinear Sci.* **7**(1), 1–26 (2022).
69. Dewasurendra, M. & Vajravelu, K. On the method of inverse mapping for solutions of coupled systems of nonlinear differential equations arising in nanofluid flow, heat and mass transfer. *Appl. Math. Nonlinear Sci.* **3**(1), 1–14 (2018).

Acknowledgements

The authors are thankful to UAEU for the financial support through the UPAR Grant Number 12S002.

Author contributions

Z.S.: Paper write up, Methodology S.B.S.: Supervision, Coding Qasem A.-M.: Reviewed the manuscript; results.

Competing interests

The authors declare no competing interests.

Additional information

Correspondence and requests for materials should be addressed to S.B.S.

Reprints and permissions information is available at www.nature.com/reprints.

Publisher's note Springer Nature remains neutral with regard to jurisdictional claims in published maps and institutional affiliations.



Open Access This article is licensed under a Creative Commons Attribution 4.0 International License, which permits use, sharing, adaptation, distribution and reproduction in any medium or format, as long as you give appropriate credit to the original author(s) and the source, provide a link to the Creative Commons licence, and indicate if changes were made. The images or other third party material in this article are included in the article's Creative Commons licence, unless indicated otherwise in a credit line to the material. If material is not included in the article's Creative Commons licence and your intended use is not permitted by statutory regulation or exceeds the permitted use, you will need to obtain permission directly from the copyright holder. To view a copy of this licence, visit <http://creativecommons.org/licenses/by/4.0/>.

© The Author(s) 2023